

New Cd Thio- and Selenocyanato Coordination Compounds and Their Impact on the Structures and Reactivity of Their Paramagnetic Counterparts

Jan Boeckmann,^[a] Inke Jeß,^[a] Thorben Reinert,^[a] and Christian Näther*^[a]

Keywords: Cadmium / Selenium / N ligands / Magnetic properties / Thermochemistry

Treatment of cadmium(II) thio- and selenocyanate with pyridazine leads to the formation of new cadmium(II) thiocyanato and selenocyanato coordination compounds [Cd(NCS)₂(pyridazine)₄] (1A), [Cd(NCSe)₂(pyridazine)₃]_n (2A), [Cd(NCS)₂(pyridazine)₂]_n (1B), [Cd(NCSe)₂(pyridazine)₂]_n (2B) and [Cd(NCS)₂(pyridazine)]_n (1C) which were characterised by single-crystal X-ray diffraction. Investigations of the thermal degradation behaviour of 1A and 2A using simultaneous differential thermoanalysis and thermogravimetry as well as X-ray powder diffraction, IR- and Raman spectroscopy prove that on heating, the pyridazine-rich compounds 1A and 2A decompose in a stepwise manner leading in the first TG step to the formation of the pyridazine-

deficient compounds [Cd(NCS)₂(pyridazine)₂]_n (1B) and [Cd(NCSe)₂(pyridazine)₂]_n (2B) as intermediates. While the selenocyanato compound decomposes on further heating, for the thiocyanato compound an additional TG step is observed, in which a pyridazine-deficient 1:1 compound of composition [Cd(NCS)₂(pyridazine)]_n (1C) is formed. The structures and thermal reactivity are discussed and compared with that of related transition metal thiocyanato and selenocyanato coordination compounds with pyridine and pyrazine as the coligand. More importantly, on the basis of these investigations, the hitherto unknown structures of the ligand-deficient paramagnetic counterparts were determined.

Introduction

Interest and investigations on coordination compounds with paramagnetic metal centres which are interlinked by means of small-sized anions and might therefore enable cooperative magnetic phenomena have continuously increased over the last years.^[1] In connection with this, azido (N₃⁻), carboxylato (RCO₂⁻, R = H, or an organic remainder) and cyanido (CN⁻) coordination compounds which show interesting magnetic behaviour like metamagnetism or slow relaxation of the magnetisation have already been reported.^[2] In this context we have reported the first thiocyanato (NCS⁻) and selenocyanato (NCSe⁻) compounds which show such behaviour.^[3,4] However, because the terminal coordination mode of these anions is energetically favoured, μ -1,3 bridging thio- and selenocyanatos of Mn, Fe, Co and Ni are sometimes difficult to prepare in solution. In this context, we have reported an alternative strategy for the rational synthesis of such compounds in which ligand-rich (ligand-rich = rich on neutral coligands) precursor compounds based on transition metal thio- or selenocyanates with only terminal bonded anions and additional neutral coligands are thermally decomposed leading to the phase-pure formation of ligand-deficient (ligand-deficient = lack-

ing neutral coligands) intermediates in which the anions become μ -1,3 bridging and can therefore mediate magnetic exchange interactions.^[5,6,7] In some cases however, the ligand-deficient compounds can also be prepared in solution and therefore crystallised and structurally characterised by single crystal X-ray diffraction but they are frequently only accessible through thermal decomposition reactions. Unfortunately this leads to the formation of microcrystalline powders with sometimes small particles and broad reflection profiles and, therefore, indexing of their powder pattern is difficult to achieve. However, this problem might be successfully overcome if compounds were prepared showing similar structural features and which consist of chalcophilic metal cations that, in contrast to terminal bonded anions, prefer a μ -1,3 bridging coordination mode. These conditions are perfectly fulfilled by coordination compounds based on Cd^{II} thio- or selenocyanate which exhibit structures that are very often comparable with that of the Mn^{II}, Fe^{II}, Co^{II} and Ni^{II} analogues.^[6,8] Due to the higher chalcophilicity of the Cd^{II} metal cations, such compounds prefer a μ -1,3 bridging coordination mode and, therefore, the corresponding ligand-deficient intermediates can easily be crystallised from solution and structurally characterised by single-crystal X-ray diffraction. If they are isotopic with their paramagnetic counterparts obtained by thermal decomposition, the structures of the latter can simply be determined by Rietveld refinement. This is one of the reasons why we have started systematic investigations of cadmium thio- and selenocyanato complexes.

[a] Institut für Anorganische Chemie, Christian-Albrechts-Universität zu Kiel, Max-Eyth-Straße 2, 24098 Kiel, Germany
Fax: +49-431-8801520
E-mail: cnaether@ac.uni-kiel.de

Supporting information for this article is available on the WWW under <http://dx.doi.org/10.1002/ejic.201100745>.

In the course of our project we also investigated corresponding compounds with pyridazine as coligand which can act as monodentate or a bidentate ligand. In the former case, only one of the two N atoms is involved in metal coordination, whereas in the latter two different metal cations are linked by the pyridazine ligand. There are a very few examples^[7,9,10] where this ligand forms 1:4 complexes and there are also examples in which both coordination modes are found in the same structure.^[11,12] Within this project we have synthesised ligand-rich compounds with Mn, Fe, Co and Ni but we were not able to obtain ligand-deficient compounds with μ -1,3 bridging anions using conventional solution synthesis. With Ni, for example, we obtained a trinuclear complex of composition $[\text{Ni}_3(\text{NCS})_6(\text{pyridazine})_6]$ in which the pyridazine coligand acts as a monodentate and bidentate ligand and, besides terminal *N*-bonded thiocyanato anions, μ -1,1 *N*-bridging anions are also found.^[12] However, a large number of ligand-deficient intermediates can easily be prepared by thermal decomposition which is the case, for example, for $[\text{Mn}(\text{NCS})_2(\text{pyridazine})_4]$. The latter transforms into three different intermediates on heating. Unfortunately we were not able to extract any structural information and we therefore decided to investigate the corresponding compounds with cadmium thio- and selenocyanate. Here we report on our investigations.

Results and Discussion

Synthetic Aspects

In order to examine the number and nature of the Cd^{II} coordination compounds that can be prepared in solution, different ratios of the metal salts and the neutral *N*-donor coligand pyridazine were combined in acetonitrile, water or pure coligand and the precipitates formed were filtered off and investigated by XRPD measurements. These experiments showed that with Cd^{II} thiocyanate, three different crystalline phases occur whereas with Cd^{II} selenocyanate only two of them can be found. The results of elemental analysis indicate that reaction of $\text{Cd}(\text{NCS})_2$ or $\text{Cd}(\text{NCSe})_2$ in pure coligand leads to the formation of a pyridazine-rich 1:4 thiocyanato compound of composition $[\text{Cd}(\text{NCS})_2(\text{pyridazine})_4]$ (**1A**) and a pyridazine-rich 1:3 selenocyanato compound of composition $[\text{Cd}(\text{NCSe})_2(\text{pyridazine})_3]_n$ (**2A**). Reaction of $\text{Cd}(\text{NCSe})_2$ with pyridazine in water and acetonitrile with a molar ratio down from 1:10 to 1:1 (ratio metal salt to coligand) results in only one crystalline phase of a pyridazine-deficient 1:2 compound of composition $[\text{Cd}(\text{NCSe})_2(\text{pyridazine})_2]_n$ (**2B**). Reaction of $\text{Cd}(\text{NCS})_2$ with pyridazine in water and acetonitrile with a molar ratio down from 1:10 to 1:2 leads to the formation of a pyridazine-deficient 1:2 compound of composition $[\text{Cd}(\text{NCS})_2(\text{pyridazine})_2]_n$ (**1B**), whereas reaction of equivalent molar amounts of $\text{Cd}(\text{NCS})_2$ with pyridazine in water and acetonitrile leads to the formation of an additional phase of composition $[\text{Cd}(\text{NCS})_2(\text{pyridazine})]_n$ (**1C**). According to the XRPD measurements, compounds **1B** and **2B** should be isotopic. Based on these results we tried to prepare single

crystals of all compounds and this can easily be performed at room-temperature or under solvothermal conditions.

Structural Investigations

Structure of the 1:4 Compound $[\text{Cd}(\text{NCS})_2(\text{pyridazine})_4]$ (**1A**)

The pyridazine-rich 1:4 compound $[\text{Cd}(\text{NCS})_2(\text{pyridazine})_4]$ (**1A**) crystallises in the centrosymmetric triclinic space group $P\bar{1}$ with one formula unit in the unit cell and is isostructural with the Co^{II} compound reported recently.^[9] The cadmium cation is located on a centre of inversion and is coordinated by six nitrogen atoms from two terminal *N*-bonded thiocyanato anions and four terminal bonded pyridazine ligands, all of them in general positions, within a slightly distorted octahedral coordination geometry (Figure 1 and Table 1).

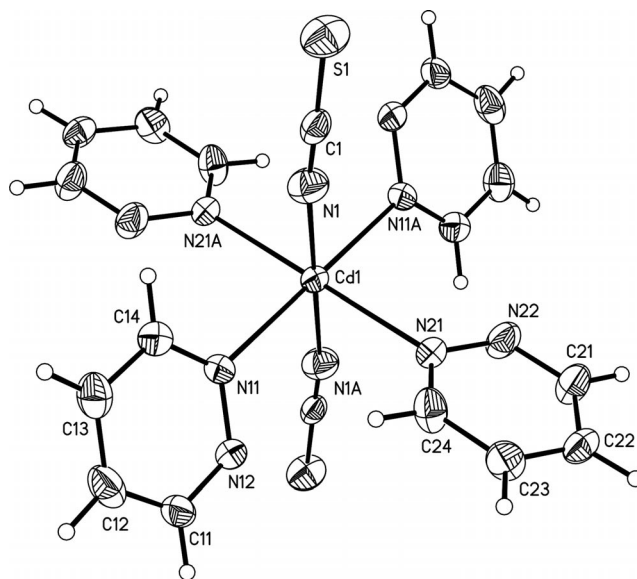


Figure 1. Molecular structure of compound **1A** with labelling and displacement ellipsoids drawn at the 50% probability level. Symmetry transformation used to generate equivalent atoms: A: $-x, -y + 1, -z + 1$. (a packing diagram is shown in Figure S1 of the Supporting Information).

Table 1. Selected bond lengths [\AA] and angles [$^\circ$] for **1A**. Symmetry code: A: $-x, -y + 1, -z + 1$.

$[\text{Cd}(\text{NCS})_2(\text{pyridazine})_4]$ (1A)			
Cd(1)–N(1)	2.287(3)	N(1)–Cd(1)–N(21)	88.06(9)
Cd(1)–N(11)	2.386(2)	N(1)–Cd(1)–N(21A)	91.94(9)
Cd(1)–N(21)	2.421(2)	N(11)–Cd(1)–N(21)	86.85(8)
N(1)–Cd(1)–N(1A)	180.0	N(11)–Cd(1)–N(21A)	93.15(8)
N(1)–Cd(1)–N(11)	85.76(10)	N(11)–Cd(1)–N(11A)	180.0
N(1)–Cd(1)–N(11A)	94.24(10)	N(21)–Cd(1)–N(21A)	180.0

The shortest metal to metal separation between the complexes amounts to 8.0308(8) \AA .

The metal–nitrogen distances range between 2.287(3) and 2.421(2) \AA and the angles around the metal cations range between 85.76(10) and 94.24(10) $^\circ$ (Table 1). In the

crystal structure, the discrete complexes are arranged into columns which are elongated in the direction of the crystallographic *b* axis and these columns are further arranged into layers in the *bc* plane (Figure S1).

Structure of the 1:3 Compound $[\text{Cd}(\text{NCSe})_2(\text{pyridazine})_3]_n$ (**2A**)

The pyridazine-rich 1:3 compound $[\text{Cd}(\text{NCSe})_2(\text{pyridazine})_3]_n$ (**2A**) crystallises in the triclinic centrosymmetric space group $P\bar{1}$ with four formula units per unit cell. The asymmetric unit consists of three cadmium cations two of which are located on a centre of inversion and one in a general position, four selenocyanato anions and six pyridazine ligands, all of them located in general positions (Figure 2).

Cd2 is coordinated by four nitrogen atoms from four terminal *N*-bonded pyridazine ligands and by two selenium atoms from two μ -1,3 bridging selenocyanato anions in a slightly distorted octahedral coordination geometry (Figure 2 and Table 2). The remaining Cd^{II} cations are each coordinated by six nitrogen atoms from two terminal *N*-bonded pyridazine ligands, two terminal *N*-bonded and two μ -1,3 bridging selenocyanato anions in a slightly distorted octahedral coordination geometry (Figure 2 and Table 2). The metal centres are bridged into polymeric chains, each through a single selenocyanato anion. These chains are elongated perpendicular to the crystallographic *a* axis. The metal–nitrogen distances range between 2.294(4) and 2.400(3) Å and the angles around the metal cations range between 86.16 (12) and 93.84 (12)° (Table 2). The shortest metal to metal intrachain separation amounts to 6.1618(6) Å, whereas the shortest metal to metal interchain separation amounts to 9.0836(12) Å.

Structures of the 1:2 Compounds $[\text{Cd}(\text{NCS})_2(\text{pyridazine})_2]_n$ (**1B**) and $[\text{Cd}(\text{NCSe})_2(\text{pyridazine})_2]_n$ (**2B**)

The pyridazine-deficient 1:2 compounds $[\text{Cd}(\text{NCS})_2(\text{pyridazine})_2]_n$ (**1B**) and $[\text{Cd}(\text{NCSe})_2(\text{pyridazine})_2]_n$ (**2B**) are isotypic and crystallise in the centrosymmetric orthorhombic

Table 2. Selected bond lengths [Å] and angles [°] for **2A**. Symmetry codes: A: $-x, -y + 1, -z + 1$; B: $-x + 1, -y, -z$.

$[\text{Cd}(\text{NCSe})_2(\text{pyridazine})_3]_n$ (2A)			
Cd(1)–N(1)	2.300(3)	N(1)–Cd(1)–N(2)	93.09(13)
Cd(1)–N(2)	2.318(3)	N(1)–Cd(1)–N(11)	93.84(12)
Cd(1)–N(11)	2.376(3)	N(2)–Cd(1)–N(11)	86.31(12)
Cd(2)–N(21)	2.388(3)	Se(2)–Cd(2)–Se(3)	178.400(16)
Cd(2)–N(31)	2.400(3)	N(21)–Cd(2)–Se(2)	89.40(7)
Cd(2)–N(41)	2.354(3)	N(21)–Cd(2)–Se(3)	92.20(7)
Cd(2)–N(51)	2.368(3)	N(31)–Cd(2)–Se(2)	91.82(7)
Cd(2)–Se(2)	2.8003(5)	N(31)–Cd(2)–Se(3)	86.58(7)
Cd(2)–Se(3)	2.8151(5)	N(21)–Cd(2)–N(31)	177.57(11)
Cd(3)–N(3)	2.322(3)	N(3)–Cd(3)–N(3B)	180.0
Cd(3)–N(4)	2.294(4)	N(3)–Cd(3)–N(61)	93.24(13)
Cd(3)–N(61)	2.371(3)	N(3)–Cd(3)–N(4)	92.56(14)
N(1)–Cd(1)–N(1A)	180.0	N(4)–Cd(3)–N(61)	89.64(13)

space group $Pnma$ with four formula units per unit cell. The asymmetric unit consists of one Cd^{II} ion and two thio- or selenocyanato anions (**1B** and **2B**, respectively) situated on a mirror plane as well as one pyridazine ligand in a general position (Figure 3).

The Cd^{II} ion is coordinated by four N atoms from two pyridazine ligands and two thio- or selenocyanato anions (**1B** and **2B**, respectively) each in a mutual *cis* orientation and by two S or Se atoms from two adjacent thio- or selenocyanato anions within a slightly distorted octahedral coordination environment (Figure 3 and Table 3). The Cd^{II} ions are μ -1,3 bridged by means of the anions into polymeric chains that are elongated in the direction of the crystallographic *a* axis. The Cd^{II}...Cd^{II} intrachain separation amounts to 5.8667(7) Å for **1B** and 6.0045(6) Å for **2B**, whereas the shortest Cd^{II}...Cd^{II} interchain separation amounts to 7.9160(8) Å for **1B** and 8.1861(7) Å for **2B**. These chains are further connected by weak S...S interactions with a separation of 3.6801(21) Å or Se...Se interactions with a separation of 3.7802(9) Å into layers which are located in the crystallographic *ac* plane.

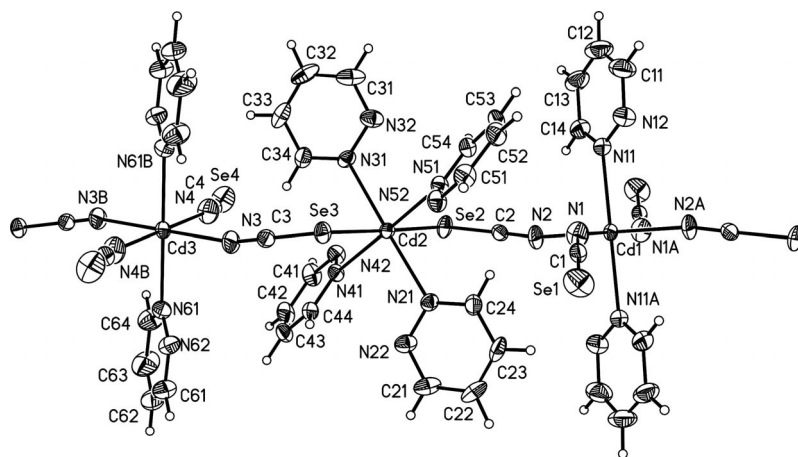


Figure 2. Molecular structure of compound **2A** with labelling and displacement ellipsoids drawn at the 50% probability level. Symmetry transformation used to generate equivalent atoms: A: $-x, -y + 1, -z + 1$; B: $-x + 1, -y, -z$. (a packing diagram of **2A** is shown in Figure S2 of the Supporting Information).

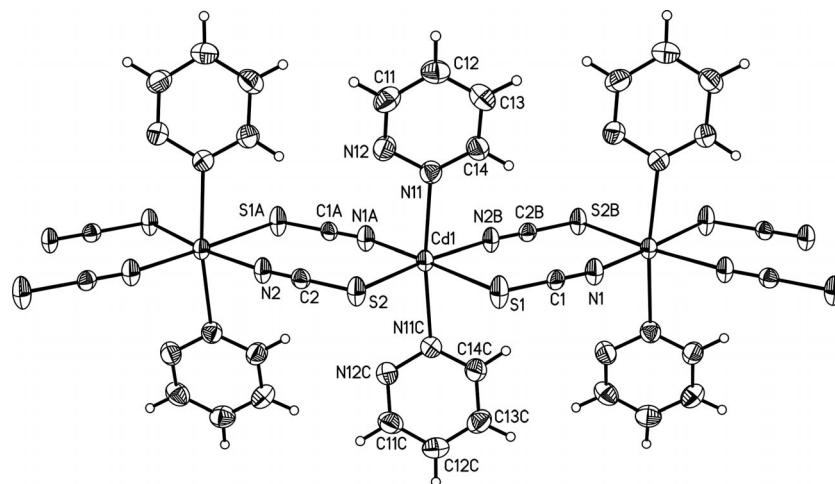


Figure 3. Molecular structure of compound **1B** as a representative example with labelling and displacement ellipsoids drawn at the 30% probability level. Symmetry transformation used to generate equivalent atoms: A: $x - 1/2, y, -z + 3/2$; B: $x + 1/2, y, -z + 3/2$; C: $x, -y + 3/2, z$. (a packing diagram of **1B** is shown in Figure S3 and an ORTEP plot of **2B** is shown in Figure S4 of the Supporting Information).

Table 3. Selected bond lengths [Å] and angles [°] for **1B** and **2B**. Symmetry code: A: $x - 1/2, y, -z + 3/2$; B: $x + 1/2, y, -z + 3/2$; C: $x, -y + 3/2, z$.

[Cd(NCS) ₂ (pyridazine) ₂] _n (1B)			
Cd(1)–S(1)	2.7931(16)	N(1A)–Cd(1)–S(1)	176.94(13)
Cd(1)–S(2)	2.6572(16)	N(1A)–Cd(1)–S(2)	97.81(13)
Cd(1)–N(1A)	2.272(5)	N(2B)–Cd(1)–N(11)	88.05(8)
Cd(1)–N(2B)	2.306(5)	N(2B)–Cd(1)–S(1)	91.04(13)
Cd(1)–N(11)	2.378(3)	N(2B)–Cd(1)–S(2)	170.17(12)
S(1)–Cd(1)–S(2)	79.13(4)	N(11)–Cd(1)–S(1)	86.64(8)
N(1A)–Cd(1)–N(2B)	92.02(17)	N(11)–Cd(1)–S(2)	91.35(8)
N(1A)–Cd(1)–N(11)	93.46(8)		
[Cd(NCSe) ₂ (pyridazine) ₂] _n (2B)			
Cd(1)–Se(1)	2.8588(7)	N(1A)–Cd(1)–Se(1)	177.17(13)
Cd(1)–Se(2)	2.7320(7)	N(1A)–Cd(1)–Se(2)	98.71(13)
Cd(1)–N(1A)	2.281(5)	N(2B)–Cd(1)–N(11)	86.73(9)
Cd(1)–N(2B)	2.332(5)	N(2B)–Cd(1)–Se(1)	92.12(12)
Cd(1)–N(11)	2.386(4)	N(2B)–Cd(1)–Se(2)	170.58(12)
Se(1)–Cd(1)–Se(2)	78.46(2)	N(11)–Cd(1)–Se(1)	88.23(9)
N(1A)–Cd(1)–N(2B)	90.71(18)	N(11)–Cd(1)–Se(2)	92.92(9)
N(1A)–Cd(1)–N(11)	91.94(9)		

Structure of the 1:1 Compound [Cd(NCS)₂(pyridazine)]_n (**1C**)

The pyridazine-deficient 1:1 compound [Cd(NCS)₂(pyridazine)]_n (**1C**) crystallises in the centrosymmetric monoclinic space group $P2_1/n$ with eight formula units per unit cell. The asymmetric unit consists of two Cd^{II} ions, four thiocyanato anions and two pyridazine ligands, all in general positions. One of the Cd^{II} ions is coordinated by four N atoms from two μ_2 -bridging pyridazine ligands, one μ -1,1 bridging and one μ -1,3 bridging thiocyanato anion, each in a mutual *cis* orientation, and by two S atoms from two adjacent μ -1,3 bridging thiocyanato anions within a distorted octahedral coordination environment (Figure 4 and Table 4). The remaining Cd^{II} ion is coordinated by five N atoms from two μ_2 -bridging pyridazine ligands, one μ -1,1 bridging and two μ -1,3 bridging thiocyanato anions, each in a mutual *cis* orientation, and by one S atom from an

adjacent μ -1,3 bridging thiocyanato anion within a distorted octahedral coordination geometry (Figure 4 and Table 4).

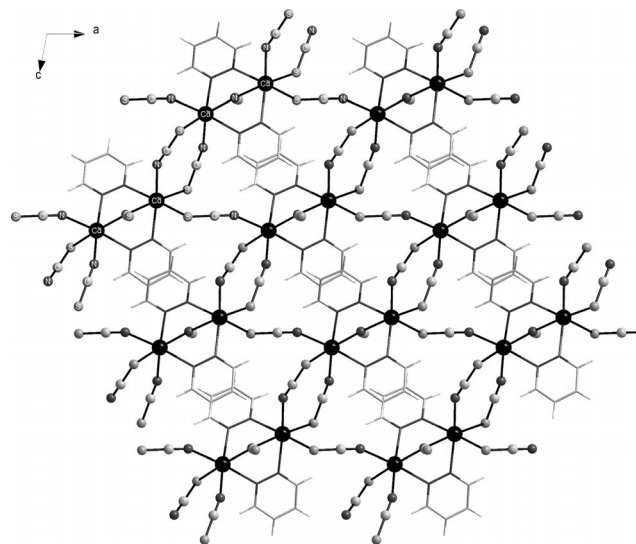


Figure 4. Packing diagram of compound **1C** viewed along the *b* axis (black = metal, dark-grey = nitrogen, light-grey = carbon, grey = sulfur, white = hydrogen) (an ORTEP plot of **1C** is shown in Figure S5 of the Supporting Information).

These dinuclear entities are further linked by means of μ -1,3 bridging thiocyanato anions into double and single chains forming a 2D layer network which is parallel to the crystallographic *ac* plane (Figure 4). The Cd^{II}...Cd^{II} separation within the dinuclear entity through the μ -1,1 bridging N-bonded thiocyanato anions amounts to 3.7598(8) Å, whereas the Cd^{II}...Cd^{II} intrachain separation through the single chain of the μ -1,3 bridging thiocyanato anions amounts to 6.5202(8) Å, and that for the double chain of the μ -1,3 bridging thiocyanato anions amounts to 5.6124(9) Å.

Table 4. Selected bond lengths [Å] and angles [°] for **1C**. Symmetry code: A: $x - 1/2, -y + 1/2, z + 1/2$; B: $x + 1/2, -y + 1/2, z - 1/2$; C: $x + 1, y, z$; D: $x - 1, y, z$.

[Cd(NCS) ₂ (pyridazine)] _n (1C)			
Cd(1)–S(1)	2.646(2)	S(1)–Cd(1)–S(2)	97.57(7)
Cd(1)–S(2)	2.674(2)	N(1B)–Cd(2)–N(2C)	92.7(2)
Cd(1)–N(3)	2.342(6)	N(1B)–Cd(2)–N(3)	91.4(2)
Cd(1)–N(4A)	2.291(7)	N(1B)–Cd(2)–S(4)	96.75(19)
Cd(1)–N(11)	2.415(7)	N(2C)–Cd(2)–N(3)	103.6(2)
Cd(1)–N(21)	2.427(6)	N(2C)–Cd(2)–S(4)	87.87(18)
Cd(2)–S(4)	2.733(2)	N(3)–Cd(1)–S(1)	169.62(17)
Cd(2)–N(1B)	2.281(8)	N(3)–Cd(1)–S(2)	88.23(17)
Cd(2)–N(2C)	2.281(6)	N(3)–Cd(2)–S(4)	165.64(16)
Cd(2)–N(3)	2.333(6)	N(4A)–Cd(1)–S(1)	97.09(18)
Cd(2)–N(12)	2.430(6)	N(4A)–Cd(1)–S(2)	88.6(2)
Cd(2)–N(22)	2.369(6)	N(4A)–Cd(1)–N(3)	91.6(2)
Cd(1)–N(3)–Cd(2)	107.1(3)		

Thermoanalytical Investigations

In order to investigate the thermal properties of the ligand-rich compounds, simultaneous DTA-TG (differential thermoanalysis and thermogravimetry) measurements were performed. On heating the pyridazine-rich compound **1A** in a thermobalance, a stepwise decomposition was observed. In the TG curve three mass steps accompanied with endothermic events in the DTA curve can be observed (Figure 5). The mass loss in the first step $\Delta m_1 = 30.6\%$ is in good agreement with that calculated for the removal of two molecules pyridazine ($\Delta m_{\text{calcd.}} = 29.2\%$) (Figure 5). The mass losses of both of the following steps of $\Delta m_2 = 15.3\%$ and $\Delta m_3 = 15.0\%$ are each in reasonable agreement with the calculated mass loss for one molecule pyridazine ($\Delta m_{\text{calcd.}} = 14.6\%$) (Figure 5). On the basis of the experimental mass losses, it can be assumed that in the first mass

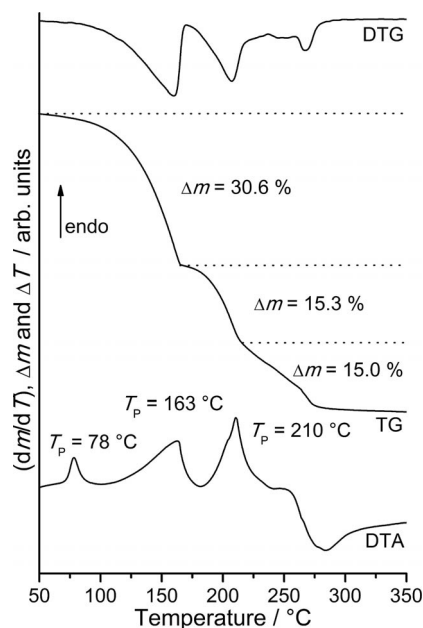


Figure 5. DTG, TG and DTA curves for compound **1A**. Heating rate: 4 °C min^{-1} ; given are the mass changes in % and the peak temperatures T_p in °C.

step Δm_1 , the formation of a pyridazine-deficient 1:2 intermediate of composition $[\text{Cd}(\text{NCS})_2(\text{pyridazine})_2]_n$ (**1B**) occurs. The second mass step Δm_2 gives further hints of the formation of a pyridazine-deficient intermediate of composition $[\text{Cd}(\text{NCS})_2(\text{pyridazine})]_n$ (**1C**) which itself decomposes on further heating (For DTG, TG and DTA curves for compounds **1B** and **1C** see Figures S6–S7 in the Supporting Information).

To verify the nature of the intermediates formed, additional TG measurements were performed and stopped after the first and second TG step. Elemental analysis of the residues obtained support the assumption of the formation of pyridazine-deficient 1:2 and 1:1 intermediates. Final XRPD investigations of the residues clearly showed that the pyridazine-deficient compounds **1B** and **1C** were formed as pure phases in the first and second TG steps (Figure 6).

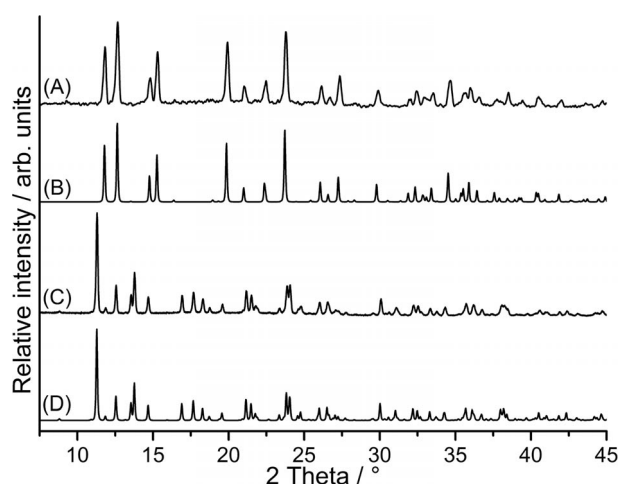


Figure 6. Experimental XRPD patterns of the intermediates obtained after the first (A) and second (C) heating step of compound **1A** together with calculated XRPD patterns for the 1:2 compound **1B** (B) and the 1:1 compound **1C** (D).

If compound **2A** is heated in a thermobalance two mass steps are observed which are not well resolved. Even heating rate dependent measurements did not improve the resolution of the thermal events (Figure S8 of the Supporting Information). The experimental mass loss in the first step of $\Delta m_1 = 14.1\%$ is in good agreement with that calculated for the removal of one molecule pyridazine ($\Delta m_{\text{calcd.}} = 14.2\%$) (Figure 7) and accompanied with an endothermic event in the DTA curve.

The experimental mass loss of the following step $\Delta m_2 = 28.3\%$ is in agreement with that calculated for the removal of two molecules pyridazine ($\Delta m_{\text{calcd.}} = 28.5\%$). Therefore, based on the experimental mass losses, it can be assumed that in the first mass step Δm_1 a pyridazine-deficient 1:2 intermediate of composition $[\text{Cd}(\text{NCS})_2(\text{pyridazine})_2]_n$ (**2B**) has formed which loses all coligands on further heating (For DTG, TG and DTA curves for compound **2B** see Figure S9 of the Supporting Information). To verify the nature of the intermediate formed, additional TG measurements were performed and stopped after the first TG step. XRPD

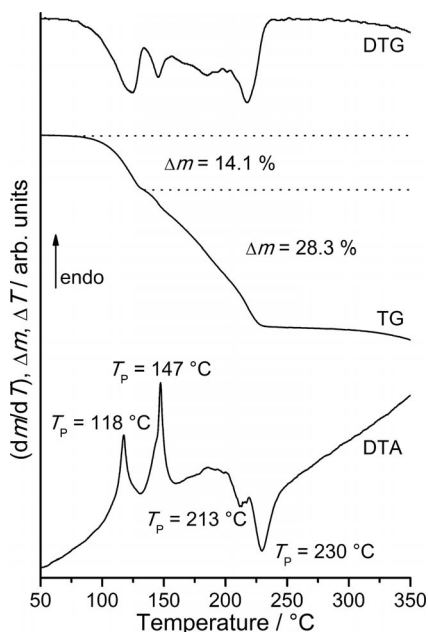


Figure 7. DTG, TG and DTA curves for compound **2A**. Heating rate: $1\text{ }^{\circ}\text{Cmin}^{-1}$; given are the mass changes in % and the peak temperatures T_p in $^{\circ}\text{C}$.

measurements showed that compound **2B** has formed but always in a mixture with the precursor **2A** and an additional unknown phase which could not be identified. It might be that a second ligand-deficient phase or a polymorphic modification forms on heating but because of the low-resolution it cannot be isolated (Figure S10 in the Supporting Information).

Spectroscopic Measurements

The coordination modes of the thiocyanato and selenocyanato anions in compounds **1A–1C** and **2A–2B** (Figure S10–S14 of the Supporting Information) can be additionally verified from their vibrational spectra and, therefore, IR and Raman spectroscopic investigations were performed. In compounds with terminal *N*-bonded thio- or selenocyanato anions, the asymmetric $\nu_{\text{as}}(\text{CN})$ is expected to be at about 2050 cm^{-1} .^[13] For μ -1,3 bridging thio- or selenocyanato anions the asymmetric $\nu_{\text{as}}(\text{CN})$ is shifted to higher wavenumbers and can be found $\geq 2100\text{ cm}^{-1}$ whereas for a μ -1,1 bridging anions the asymmetric $\nu_{\text{as}}(\text{CN})$ is shifted to lower wavenumbers and can be found $\leq 2000\text{ cm}^{-1}$. However, even if the coordination mode is clear from our structural investigations, such measurements can be especially helpful in the cases in which no structural information can be retrieved from diffraction experiments. In this context it must be kept in mind that the spectroscopic values mentioned above are based in part on old results and we have found that exceptions from these exact numbers are very often discovered. Therefore, such investigations are of general interest.

These results are in full agreement with our spectroscopic investigations in which, for the pyridazine-rich 1:4 com-

pound **1A**, only one band may be observed in the IR spectrum with a value which is characteristic for terminal *N*-bonded thiocyanato anions (Table 5). For the pyridazine-rich 1:3 compound **2A**, two bands may be observed in the IR and Raman spectra which support the occurrence of both terminal *N*-bonded and μ -1,3 bridging selenocyanato anions (Table 5).

Table 5. Stretching vibration $\nu(\text{CN})$ in the IR and Raman spectra for the thio- and selenocyanato anions in compounds **1A–1C** and **2A–2B**.

Compound	IR bands [cm^{-1}]	Raman bands [cm^{-1}]
1A	2061	–
1B	2099 and 2105	2097 and 2105
1C	1985, 2094 and 2105	1985, 2093 and 2105
2A	2062 and 2113	2067 and 2117
2B	2097 and 2107	2105 and 2111

The values found in the IR and Raman spectra for the pyridazine-deficient compounds **1B** and **2B** are consistent with that expected for μ -1,3 bridging anions (Table 5). For the most pyridazine-deficient compound **1C**, values for $\nu(\text{CN})$ are observed in the IR and Raman spectra which are characteristic and consistent with μ -1,3 bridging and μ -1,1 bridging thiocyanato anions (Table 5).

General Discussion of the Structures and Reactivity

In this contribution, Cd^{II} thiocyanato and selenocyanato coordination compounds based on pyridazine as a coligand were investigated in order to compare their structural and chemical properties with those found for the corresponding coordination polymers with pyridine and pyrazine as coligands as well as Cd, Mn, Fe, Co and Ni as counter cations.

With Cd^{II} thiocyanate, a pyridazine-rich 1:4 compound of composition $[\text{Cd}(\text{NCS})_2(\text{pyridazine})_4]$ (**1A**) was observed consisting of discrete complexes that are identical to those in $[\text{M}(\text{NCS})_2(\text{pyridine})_4]$ ($\text{M} = \text{Mn}, \text{Fe}, \text{Co}, \text{Ni}$ and Cd) reported recently.^[14] Consequently, similar reactivity is observed such that on heating a transformation into a ligand-deficient intermediate of composition $[\text{Cd}(\text{NCS})_2(\text{pyridazine})_2]_n$ (**1B**) is observed and this intermediate can also be isolated for the compounds with pyridine. In contrast to the pyridine compounds, an additional pyridazine-deficient compound of composition $[\text{Cd}(\text{NCS})_2(\text{pyridazine})]_n$ (**1C**) can be observed in which the metal cations are additionally bridged by the coligand.

In contrast, with Cd^{II} selenocyanate, no ligand-rich 1:4 compound with sixfold N coordination could be prepared and the most pyridazine-rich compound is represented by a 1:3 compound (**2A**) which shows alternating sixfold and fourfold N coordination. The reason for this behaviour can be traced back to the fact that Se is much softer than S and, therefore, with the chalcophilic and soft Cd cations Se coordination is preferred. In this context it must be mentioned that the structure of **2A** in which the metal cations are linked by only one anion is quite unusual and without

any precedence in the literature. In most cases the metal(II) cations are linked by two thio- or selenocyanato anions into chains which is also observed, for example, with azido anions. As expected, on heating the 1:3 compound **2A**, a transformation into the 1:2 compound **2B** can be observed which is isotypic with **1B** and which consists of a 1D coordination polymer in which the metal cations are each linked by two μ -1,3 bridging anions. Therefore, the structure of the 1:3 compound **2A** represents a structural intermediate between the discrete 1:4 compound and the 1D 1:2 compounds which are frequently observed with all monodentate ligands. Interestingly, if the crystal structures of all compounds are compared, a smooth reaction pathway can be found from the ligand-rich structure transformation into the ligand-deficient intermediates. However, the reason why a 1:3 compound is not observed in the thermal decomposition reaction of the 1:4 pyridazine compound is unclear. From previous investigations we know that the kinetics of the different reactions might play a role and that different products can be observed on heating rate dependent measurements, for example.^[15] Therefore, it might be that such 1:3 compounds were overlooked. In any case, the results clearly show that even such simple reactions are much more complicated to understand and might proceed by means of additional metastable intermediates that are sometimes difficult to identify.

Moreover, differences between sulfur and selenium were also obvious because only with thiocyanate can a 1:1 compound (**1C**) be observed. In this structure, the pyridazine coligand becomes μ -1,2 bridging and one of the thiocyanato anions becomes μ -1,1 bridging and, therefore, the number of Cd–N bonds increases. Consequently, in the case of thiocyanate it can be assumed that the difference between *N*- and *S*-bonding is not as pronounced as it is the case for *Se*-bonding and therefore the formation of a ligand-deficient 1:1 selenocyanato compound is suppressed.

Impact on the Structures of the Paramagnetic Counterparts

Based on our results, it is indicated that the cadmium thio- and selenocyanato coordination polymers show similar structural and thermal behaviour to that of the paramagnetic cations but, in contrast, the latter prefer a bridging instead of a terminal coordination. Consequently, ligand-deficient compounds with Cd might be easily crystallised and these compounds can act as structural models for the corresponding paramagnetic ligand-deficient intermediates in those cases where they are isotypic. In this context we wish to mention that coordination compounds with pyridazine and the paramagnetic metals Mn, Fe, Co and Ni are currently being investigated in our group. With these metal cations, only the ligand-rich 1:4 compounds can be prepared in solution whereas ligand-deficient intermediates are not accessible. This is disappointing because, especially in these compounds, cooperative magnetic phenomena might be observed. However, first results for the Mn compound show that on heating, a transformation of the 1:4

compound into a 1:1 compound through additional intermediates can be observed. Unfortunately the powder patterns of these intermediates are of low quality and, as a result, no structural information can be extracted. However, based on the results of this work we have found that the powder pattern of the 1:1 Mn compound is very similar to that of the Cd compound **1C**. To substantiate this comparison we determined the structure of the 1:1 intermediate obtained from thermal decomposition by Rietveld refinement based on the structural data of compound **1C** (Figure S21 and Table S1 of the Supporting Information). If the calculated pattern for the Mn compound is compared with that of the intermediate and that of compound **1C** it is obvious that $[\text{Mn}(\text{NCS})_2(\text{pyridazine})]_n$ has formed in the thermal decomposition reaction and that this compound is isotypic with **1C** (Figure 8).

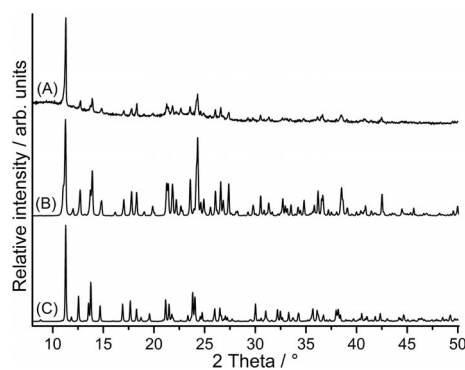


Figure 8. Experimental XRPD pattern of the intermediate obtained after the second heating step of compound $[\text{Mn}(\text{NCS})_2(\text{pyridazine})_4]$ (A) together with calculated XRPD patterns for the 1:1 compound $[\text{Mn}(\text{NCS})_2(\text{pyridazine})]_n$ (B) and the 1:1 compound $[\text{Cd}(\text{NCS})_2(\text{pyridazine})]_n$ (**1C**) (C).

Conclusion

Our approach to use the diamagnetic cadmium thio- and selenocyanates as structural models for their paramagnetic counterparts seems to be very fruitful. It could be shown that changing the metal source from the harder metals such as Mn, Fe, Co and Ni to Cd results in the formation of ligand-deficient compounds with higher condensed networks, one of which is isotypic with its paramagnetic counterpart. This seems to be one of the most important results of our investigations which is of extraordinary importance for future work in which we will systematically investigate the magnetic properties of such materials. In this context we would like to mention that we have prepared several ligand-deficient intermediates of different stoichiometry with different monodentate ligands by thermal decomposition but most of their structures are still unknown. It is highly likely that several of them are isotypic either with their Cd-based thio- or selenocyanato analogues. Therefore, the preparation and characterisation of the corresponding Cd compounds will be the subject of our future investigations.

Experimental Section

Syntheses: Cd(NO₃)₂·4H₂O and CdSO₄·8H₂O were obtained from Merck. KNCS, Ba(NCS)₂·3H₂O and pyridazine were obtained from Alfa Aesar. Solvents were used without further purification. Crystalline powders of compounds **1A–1C** and **2A–2B** were prepared by stirring the reactants in appropriate solvents at room temperature. The residues of **1B–1C** and **2A–2B** were filtered off and washed with ethanol and diethyl ether and dried in air. The resultant precipitate of **1A** is air sensitive and has to be kept in the mother liquor. The purity of all compounds was checked by X-ray powder diffraction (see Figures S16 – S20 in the Supporting Information) and elemental analysis.

Cd(NCS)₂: Ba(NCS)₂·3H₂O (3.0755 g, 10 mmol) and CdSO₄·8H₂O (3.5258 g, 10 mmol) were stirred in water (100 mL). The colourless precipitate of BaSO₄ was filtered off and the water was removed from the filtrate by heating. The final product was dried at 80 °C. The homogeneity of the product was investigated by X-ray powder diffraction. Cd(NCS)₂ (228.6): calcd. C 10.5, N 12.3, S 28.1; found C 10.4, N 12.1, S 27.9.

Synthesis of Compound 1A: Cd(NCS)₂ (114 mg, 0.50 mmol) and pyridazine (725 µL, 10.00 mmol) were stirred together in a 3 mL snap cap vial for 3 d. Single crystals suitable for single-crystal X-ray diffraction were prepared by the same method but with stirring omitted. IR (KBr): $\tilde{\nu}$ = 2061 (m), 1655 (w), 1563 (m), 1444 (w), 1412 (m), 1282 (w), 1182 (m), 1108 (m), 1061 (m), 1023 (m), 961 (s), 754 (s), 665 (w), 615 (w) cm⁻¹. C₁₈H₁₆CdN₁₀S₂ (548.9): calcd. C 39.4, H 2.9, N 25.5, S 11.7; found C 39.2, H 2.6, N 25.3, S 11.5.

Synthesis of Compound 1B: Cd(NCS)₂ (114 mg, 0.50 mmol) and pyridazine (160 µL, 2.00 mmol) were stirred together in acetonitrile (2 mL) at room temp. in a 3 mL snap cap vial for 3 d. Single crystals suitable for single-crystal X-ray diffraction were prepared by the reaction of Cd(NCS)₂ (57 mg, 0.25 mmol) and pyridazine (36 µL, 0.50 mmol) in acetonitrile (2 mL) and heating to 120 °C for 4 d. C₁₀H₈CdN₆S₂ (388.8): calcd. C 30.9, H 2.1, N 21.6, S 16.5; found C 30.6, H 2.0, N 21.4, S 16.3. IR (KBr): $\tilde{\nu}$ = 2121 (s), 2100 (s), 1570 (m), 1450 (w), 1414 (m), 1396 (w), 1288 (w), 1182 (w), 1071 (m), 970 (m), 931 (w), 914 (w), 763 (m), 746 (m), 668 (w) cm⁻¹.

Synthesis of Compound 1C: Cd(NCS)₂ (114 mg, 0.50 mmol) and pyridazine (36 µL, 0.50 mmol) were stirred together in acetonitrile (2 mL) in a 3 mL snap cap vial at room temp. for 3 d. Single crystals suitable for single-crystal X-ray diffraction were prepared by the reaction of Cd(NCS)₂ (114 mg, 0.50 mmol) and pyridazine (36 µL, 0.50 mmol) in acetonitrile (2 mL) and heating to 130 °C. After 4 d colourless needles were obtained in a mixture with compound **1B**. C₆H₄CdN₄S₂ (308.7): calcd. C 23.4, H 1.3, N 18.2, S 20.8; found C 23.4, H 1.3, N 18.1, S 20.7. IR (KBr): $\tilde{\nu}$ = 2128 (s), 2106 (s), 2100 (s), 2093 (s), 1985 (s), 1937 (w), 1576 (m), 1455 (w), 1420 (m), 1400 (w), 1296 (w), 1073 (m), 984 (m), 770 (m), 670 (w) cm⁻¹.

Synthesis of Compound 2A: Cd(NO₃)₂·4H₂O (77 mg, 0.25 mmol), KNCS (65 mg, 0.45 mmol) and pyridazine (400 µL, 5.00 mmol) were stirred together in a 3 mL snap cap vial at room temp. for 3 d. Single crystals suitable for single-crystal X-ray diffraction were prepared by the same method but without stirring. C₁₄H₁₂CdN₈Se₂ (562.6): calcd. C 29.8, H 2.1, N 19.9; found C 29.6, H 2.1, N 19.8. IR (KBr): $\tilde{\nu}$ = 2113 (s), 2062 (s), 1568 (m), 1448 (w), 1414 (s), 1385 (w), 1291 (w), 1285 (w), 965 (s), 759 (s), 741 (s), 667 (m) cm⁻¹.

Synthesis of Compound 2B: Cd(NO₃)₂·4H₂O (154 mg, 0.50 mmol), KNCS (144 mg, 1.00 mmol) and pyridazine (72.4 µL, 1.00 mmol) were stirred together in a 3 mL snap cap vial in water (2.9 mL) at

room temp. for 3 d. Single crystals suitable for single-crystal X-ray diffraction were prepared by the same method but without stirring. C₁₀H₈CdN₆Se₂ (482.5): calcd. C 24.8, H 1.6, N 17.4; found C 24.6, H 1.5, N 17.2. IR (KBr): $\tilde{\nu}$ = 2121 (s), 2108 (s), 1624 (wb), 1573 (m), 1569 (m), 1454 (w), 1449 (w), 1414 (m), 1394 (w), 1287 (w), 1068 (m), 989 (w), (m), 969 (m), 762 (m), 745 (w), 674 (w), 667 (w) cm⁻¹.

Elemental Analysis of the Residues Obtained in the Thermal Decomposition: These were isolated in the first and second heating step (see thermoanalytical investigations) of compound **1A**. Calculated for the ligand-deficient compound **1B**: C₁₀H₈CdN₆S₂ (388.8): calcd. C 30.9, H 2.1, N 21.6, S 16.5; found C 30.8, H 2.2, N 21.5, S 16.4%. Calculated for the ligand-deficient compound **1C**: C₆H₄CdN₄S₂ (308.7): calcd. C 23.4, H 1.3, N 18.2, S 20.8; found C 23.2, H 1.1, N 17.9, S 20.5.

Single-Crystal Structure Analyses: All investigations were performed with an imaging plate diffraction system from STOE & CIE (IPDS-1 for **1A**, 2A/IPDS-2 for **1B**, **1C** and **2B**) utilising Mo-*K*_α radiation. The structure solution was performed with direct methods using SHELXS-97^[16] and structure refinements were performed against *F*² using SHELXL-97.^[16] All non-hydrogen atoms were refined with anisotropic displacement parameters. The hydrogen atoms were positioned with idealised geometries and were refined with fixed isotropic displacement parameters [*U*_{iso}(H) = -1.2·*U*_{eq}(C)] using a riding model. For compound **2A**, a pseudo translation could be found which might indicate that a wrong unit cell was selected. Therefore, we tried to refine the structure in a smaller unit cell in which this pseudo translation is absent but this was unsuccessful because most parts are completely disordered. A closer look at the structure model clearly shows that this pseudo translation is only fulfilled for a few atoms. However, even from Figure 2 it is completely obvious that the torsion of the phenyl rings is completely different and that no smaller unit can be found. Details of the structure determination are given in Table 6.

CCDC-835853 (for **1A**), -835852 (for **1B**), -835854 (for **1C**), -835855 (for **2A**) and -835856 (for **2B**) contain the supplementary crystallographic data for this paper. These data can be obtained free of charge from The Cambridge Crystallographic Data Centre via www.ccdc.cam.ac.uk/data_request/cif.

Spectroscopy: Fourier transform IR spectra were recorded on a Genesis series FTIR spectrometer from ATI Mattson in KBr pellets as well on an Alpha IR spectrometer from Bruker equipped with a Platinum ATR QuickSnap™ sampling module between 4000–375 cm⁻¹. Raman spectra were recorded using a Bruker ISF66 FRA106 between 3500–100 cm⁻¹.

Elemental Analysis: CHNS analyses were performed using an EURO EA elemental analyser manufactured by EURO VECTOR Instruments and Software.

X-Ray Powder Diffraction (XRPD): XRPD experiments were performed using a STOE Transmission Powder Diffraction System (STADI P) with Cu-*K*_α radiation (λ = 154.0598 pm) and equipped with a linear position-sensitive detector (Delta 2 θ = 6.5–7° simultaneous; scan range overall: 2–130°) from STOE & CIE and an Image Plate Detector (scan range overall: 0–127°).

Differential Thermal Analysis and Thermogravimetry: The DTA-TG measurements were performed in a nitrogen atmosphere (purity: 5.0) in Al₂O₃ crucibles using a STA-409CD thermobalance from Netzsch. All measurements were performed with a flow rate of 75 mL min⁻¹ and were corrected for buoyancy and current effects. The instrument was calibrated using standard reference materials.

Table 6. Selected crystal data and details on the structure determinations for compounds **1A–1C** and **2A–2B**.

	1A	1B	1C	2A	2B
Formula	C ₁₈ H ₁₆ CdN ₁₀ S ₂	C ₁₀ H ₈ CdN ₆ S ₂	C ₆ H ₄ CdN ₄ S ₂	C ₁₄ H ₁₂ CdN ₈ Se ₂	C ₁₀ H ₈ CdN ₆ Se ₂
MW [g mol ⁻¹]	548.93	388.74	308.65	562.64	482.54
Crystal system	triclinic	orthorhombic	monoclinic	triclinic	orthorhombic
Space group	P $\bar{1}$	Pnma	P2 ₁ /n	P $\bar{1}$	Pnma
a [Å]	8.0308(8)	11.6044(8)	9.6590(6)	12.4219(9)	11.8634(5)
b [Å]	8.7489(8)	15.0009(15)	15.6860(9)	12.9662(9)	15.0230(6)
c [Å]	8.9443(9)	7.9160(5)	13.3289(9)	13.2628(10)	8.1861(3)
α [°]	84.641(11)	90.0	90.0	62.037(8)	90.0
β [°]	67.701(11)	90.0	101.152	87.134(9)	90.0
γ [°]	75.313(11)	90.0	90.0	85.820(9)	90.0
V [Å ³]	562.44(9)	1377.99(19)	1981.3(2)	1881.5(2)	1458.96(10)
T [K]	170	293	293	200	293
Z	1	4	8	4	4
D _{calcd.} [g cm ⁻³]	1.621	1.874	2.069	1.986	2.197
μ [mm ⁻¹]	1.184	1.881	2.582	5.044	6.481
θ_{max} [°]	27.98	25.98	25.00	27.00	28.00
Measured reflections	5123	4654	15379	21455	18136
R _{int}	0.0556	0.0436	0.0612	0.0404	0.0325
Unique reflections	2640	1403	3492	8025	1806
Reflections [$F_o > 4\sigma(F_o)$]	2396	1119	2671	6002	1675
Parameters	143	97	235	455	97
R ₁ [$F_o > 4\sigma(F_o)$]	0.0356	0.0362	0.0602	0.0335	0.0377
wR ₂ [all data]	0.0904	0.0624	0.0767	0.0878	0.0754
GOF	0.986	1.105	1.268	1.024	1.231
$\Delta\rho_{\text{max./min.}}$ [e Å ⁻³]	0.791/−1.045	0.426/−0.575	0.451/−0.628	0.888/−1.308	0.846/−0.705

Supporting Information (see footnote on the first page of this article): ORTEP plots, Infrared and Raman spectra and experimental and calculated XRPD patterns for compounds **1A–1C** and **2A–2B**.

Acknowledgments

This project was supported by the Deutsche Forschungsgemeinschaft (DFG) (project number NA 720/3-1) and the State of Schleswig-Holstein. We thank Professor Dr. Wolfgang Bensch for access to his experimental facility.

- [1] C. Janiak, *Dalton Trans.* **2003**, 2781–2804; D. MasPOCH, D. Ruiz-Molina, J. Veciana, *J. Mater. Chem.* **2004**, *14*, 2713–2723; A. Y. Robin, K. M. Fromm, *Coord. Chem. Rev.* **2006**, *250*, 2127–2157; D. MasPOCH, D. Ruiz-Molina, J. Veciana, *Chem. Soc. Rev.* **2007**, *36*, 770–818.
- [2] X.-Y. Wang, H.-Y. Wei, Z.-M. Wang, Z.-D. Chen, S. Gao, *Inorg. Chem.* **2005**, *44*, 572–583; X. Y. Wang, B. L. Li, X. Zhu, S. Gao, *Eur. J. Inorg. Chem.* **2005**, 3277–3286; P.-L. Yuan, P.-Z. Li, Q.-F. Sun, L.-X. Liu, K. Gao, W.-S. Liu, X.-M. Lu, S.-Y. Yu, *J. Mol. Struct.* **2008**, *890*, 112–115; M.-H. Zeng, Y.-L. Zhou, W.-X. Zhang, M. Du, H.-L. Sun, *Cryst. Growth Des.* **2009**, *9*, 20–24; D. Zhang, H. Wang, Y. Chen, Z.-H. Ni, L. Tian, J. Jiang, *Inorg. Chem.* **2009**, *48*, 11215–11225; Y.-Z. Zhang, B.-W. Wang, O. Sato, S. Gao, *Chem. Commun.* **2010**, 46, 6959–6961; V. Costa, R. Lescouëzec, J. Vaissermann, P. Herson, Y. Journaux, M. H. Araujo, J. M. Clemente-Juan, F. Lloret, M. Julve, *Inorg. Chim. Acta* **2008**, *361*, 3912–3918; R. Gheorghe, A. M. Madalan, J.-P. Costes, W. Wernsdorfer, M. Andruh, *Dalton Trans.* **2010**, *39*, 4734–4736; Z. He, Z.-M. Wang, S. Gao, C.-H. Yan, *Inorg. Chem.* **2006**, *45*, 6694–6705; B.-W. Hu, J.-P. Zhao, Q. Yang, X.-F. Zhang, M. Evangelisti, E. C. Sanudo, X.-H. Bu, *Dalton Trans.* **2010**, *39*, 11210–11217; Q.-X. Jia, H. Tian, J.-Y. Zhang, E.-Q. Gao, *Chem. Eur. J.* **2011**, *17*, 1040–1051; Z.-X. Li, Y.-F. Zeng, H. Ma, X.-H. Bu, *Chem. Commun.* **2010**, 46, 8540–8542; T.-F. Liu, D. Fu, S. Gao, Y.-Z. Zhang, H.-L. Sun, G. Su, Y.-J. Liu, *J. Am. Chem. Soc.* **2003**, *125*, 13976–13977; H.-L. Sun, Z.-M. Wang, S. Gao, *Chem. Eur. J.* **2009**, *15*, 1757–1764; L. M. Toma, R. Lescouëzec, J. Pasan, C. Ruiz-Perez, J. Vaissermann, J. Cano, R. Carrasco, W. Wernsdorfer, F. Lloret, M. Julve, *J. Am. Chem. Soc.* **2006**, *128*, 4842–4853; J. H. Yoon, D. W. Ryu, H. C. Kim, S. W. Yoon, B. Suh, C. Hong, *Chem. Eur. J.* **2009**, *15*, 3661–3665.
- [3] J. Boeckmann, C. Näther, *Dalton Trans.* **2010**, *39*, 11019–11026; J. Boeckmann, C. Näther, *Chem. Commun.* **2011**, *47*, 7104–7106.
- [4] S. Wöhlert, J. Boeckmann, M. Wriedt, C. Näther, *Angew. Chem.* **2011**, *123*, 7053–7056.
- [5] J. Boeckmann, M. Wriedt, C. Näther, *Eur. J. Inorg. Chem.* **2010**, 1820–1828; M. Wriedt, C. Näther, *Z. Anorg. Allg. Chem.* **2009**, *635*, 1115–1122; M. Wriedt, C. Näther, *Z. Anorg. Allg. Chem.* **2009**, *636*, 569–575; M. Wriedt, C. Näther, *Chem. Commun.* **2010**, *46*, 4707–4709; M. Wriedt, C. Näther, *Dalton Trans.* **2011**, *40*, 886–898; M. Wriedt, S. Sellmer, C. Näther, *Dalton Trans.* **2009**, 7975–7984.
- [6] M. Wriedt, I. Jeß, C. Näther, *Eur. J. Inorg. Chem.* **2009**, 1406–1413.
- [7] M. Wriedt, S. Sellmer, C. Näther, *Inorg. Chem.* **2009**, *48*, 6896–6903.
- [8] J. Boeckmann, T. Reinert, I. Jeß, C. Näther, *Z. Anorg. Allg. Chem.* **2011**, *637*, 1137–1144; J. Boeckmann, T. Reinert, C. Näther, *Z. Anorg. Allg. Chem.* **2011**, *637*, 940–946.
- [9] F. Lloret, G. De Munno, M. Julve, J. Cano, R. Ruiz, A. Caneschi, *Angew. Chem.* **1998**, *110*, 143; *Angew. Chem. Int. Ed.* **1998**, *37*, 135–138.
- [10] P. J. Derry, X. Wang, B. W. Smucker, *Acta Crystallogr., Sect. E* **2008**, *64*, m1449; P. A. Koz'min, T. B. Larina, M. D. Surazhskaya, A. N. Zhilyaev, G. N. Kuznetsova, *Russ. J. Inorg. Chem.* **1993**, *38*, 859; A. Novak, S. W. Keller, *J. Chem. Crystallogr.* **1997**, *27*, 279; T. Otieno, S. J. Rettig, R. C. Thompson, J. Trotter, *Inorg. Chem.* **1995**, *34*, 1718–1725; F. Allen, *Acta Crystallogr. B* **2002**, *58*, 380–388 (CSD, **2010**, version 5.32).
- [11] J. Cano, G. De Munno, F. Lloret, M. Julve, *Inorg. Chem.* **2000**, *39*, 1611–1614.
- [12] M. Wriedt, C. Näther, *Z. Anorg. Allg. Chem.* **2009**, *635*, 2459–2464.
- [13] R. A. Bailey, S. L. Kozak, T. W. Michelsen, W. N. Mills, *Coord. Chem. Rev.* **1971**, *6*, 407–445.

- [14] Y. Qu, Z.-D. Liu, H.-L. Zhu, M.-Y. Tan, *Acta Crystallogr., Sect. E* **2004**, *60*, m1013; F. Valach, P. Sivy, B. Koren, *Acta Crystallogr., Sect. C* **1984**, *40*, 957–959; I. Søtofte, E. R. Rasmussen, *Acta Chem. Scand.* **1967**, *21*, 2028–2040; H. Hartl, I. Brudgam, *Acta Crystallogr., Sect. B* **1980**, *36*, 162–165; H. Yang, Y. Chen, D. Li, D. Wang, *Acta Crystallogr., Sect. E* **2007**, *63*, m3186.
- [15] C. Näther, I. Jeß, *J. Solid State Chem.* **2002**, *169*, 103–112; C. Näther, G. Bhosekar, I. Jeß, *Inorg. Chem.* **2007**, *46*, 8079–8087.
- [16] G. M. Sheldrick, *Acta Crystallogr., Sect. A* **2008**, *64*, 112–122.

Received: July 18, 2011

Published Online: November 10, 2011